# Centrality and energy dependence of rapidity correlation patterns in relativistic heavy ion collisions*

LE Tian(乐天)[1] XU Ming-Mei(许明梅)[1,2;1)] WU Yuan-Fang(吴元芳)[1,2]

[1] Institute of Particle Physics, Huazhong Normal University, Wuhan 430079, China
[2] Key Lab of Quark and Lepton Physics (Huazhong Normal University), Ministry of Education, Wuhan 430079, China

**Abstract:** The centrality and energy dependence of rapidity correlation patterns are studied in Au+Au collisions by using AMPT with string melting, RQMD and UrQMD models. The behaviors of the short-range correlation (SRC) and the long-range correlation (LRC) are presented clearly by two spatial-position dependent correlation patterns. For centrality dependence, UrQMD and RQMD give similar results as those in AMPT, i.e., in most central collisions, the correlation structure is flatter and the correlation range is larger, which indicates a long range rapidity correlation. A long range rapidity correlation showing up in RQMD and UrQMD implies that parton interaction is not the only source of long range rapidity correlations. For energy dependence, AMPT with string melting and RQMD show quite different results. The correlation patterns in RQMD at low collision energies and those in AMPT at high collision energies have similar structures, i.e. a convex curve, while the correlation patterns in RQMD at high collision energies and those in AMPT at low collision energies show flat structures, having no position dependence. Long range rapidity correlation presents itself at high energy and disappears at low energy in RQMD, which also indicates that long range rapidity correlations may come from some trivial effects, rather than the parton interactions.

**Key words:** correlation patterns, rapidity, short-range correlation, long-range correlation

**PACS:** 25.75.-q, 13.85.Hd, 89.75.Fb **DOI:** 10.1088/1674-1137/35/3/009

## 1 Introduction

Correlations are powerful tools for exploring the complex dynamical mechanisms of multi-particle systems. For example, the momentum correlation between identical particles gives the shape of the emitting source [1], the power law behavior of the correlation strength with diminishing correlation length implies a self-similar multifractal [2], the narrowing of balance function gives hints for quark gluon plasma (QGP) formation [3], the measurement of forward-backward rapidity correlation supports parton-parton interactions in heavy ion collisions [4], and so on.

Various definitions of correlation appear one after another. Most of them care about the behaviors of the correlation strength with the correlation length, like those just mentioned above. The correlation observables having the same correlation length but different spatial positions are averaged [2, 5]. The spatial position dependence of correlations is therefore neglected, and the space structure of the correlations is smoothed out by this average procedure.

Different from the traditional measures, two spatial-position dependent correlations, i.e. neighboring bin and fixed-to-arbitrary bin correlation patterns, are suggested [6], which can reflect the dependence not only on the correlation length but also on the spatial position. The definition is

$$C_{m_1,m_2} = \frac{\langle n_{m_1} n_{m_2}\rangle}{\langle n_{m_1}\rangle\langle n_{m_2}\rangle} - 1, \qquad (1)$$

where $m_1$ and $m_2$ are the positions of two bins in phase space and $n_m$ is the multiplicity in $m$th bin. If we let $m_1 = m$ and $m_2 = m + 1$, $C_{m,m+1}$ becomes the neighboring bin correlation pattern. If we fix $m_1$ at $m_0$, and let $m_2$=$m$ be arbitrary, $C_{m_0,m}$ becomes the fixed-to-arbitrary bin correlation pattern.

The position dependence of rapidity correlation patterns has been studied by using PYTHIA for p+p collisions, AMPT and RQMD for Au+Au collisions,

Received 5 July 2010

∗ Supported by National Natural Science Foundation of China (10775056, 10835005, 11005054)

1) E-mail: xumm@iopp.ccnu.edu.cn

respectively, at $\sqrt{s_{\rm NN}}$=200 GeV [7, 8]. The position dependence of correlation in both nucleon-nucleon collision and nucleus-nucleus collision are observed. Results show that the rapidity correlation patterns in p+p collision and Au+Au collision are quite different. For Au+Au collisions, models with different particle production mechanisms give different correlation patterns, which indicates that the correlation patterns are sensitive to particle production mechanisms.

It is also argued in Ref. [6] that if QGP is formed in a relativistic heavy ion collision, the correlation between final state particles is expected to extend to larger space, and the correlation will be less dependent on the positions of the bins. Based on this argument, the position dependence of rapidity correlation patterns in central collisions in AMPT [8] shows a flat structure, which supports the QGP formation.

On the other hand, experiment at relativistic heavy ion collider (RHIC) observed long range rapidity correlation in central Au+Au collisions through the measurements on forward-backward multiplicity correlation [4] and the relative correlations of particle pairs on the difference variables $\Delta\eta$ (pseudorapidity) and $\Delta\phi$ (azimuth) (a elongated peak at nearside, usually called ridge) [9]. The dual parton model (DPM) and the color glass condensate (CGC) argue that the long range rapidity correlations observed are due to multiple parton interactions. Another model called PACIAE based on parton and hadron cascade can also give the long range rapidity correlation in central collision [10]. It supports that the long range rapidity correlation originates from parton interaction.

In this paper, we use the correlation patterns to further study the position dependence of rapidity correlation in different underlying dynamical models, so as to try to understand the correlation patterns from different physical mechanisms, as well as the source of the long range rapidity correlation. In Section 2, the centrality dependences of rapidity correlation patterns by using different Monte Carlo models AMPT, RQMD and UrQMD are compared and discussed. By the way, the energy dependences of rapidity correlation patterns, from energy $\sqrt{s_{\rm NN}}$=200 GeV to 7.7 GeV, are discussed in Section 3. A summary is given in Section 4.

## 2 Centrality dependence of rapidity correlation patterns

### 2.1 Brief introduction to monte carlo models

AMPT (a multi-phase transport model) [11] includes parton and hadron interactions. In this paper, we choose AMPT with string melting (version 2.11) in which an excited string fragments to partons. RQMD (relativistic quantum molecular dynamical model) [12] is a hadron-based transport model. A hadron rescattering mechanism can be conveniently switched on or off. We choose RQMD with re-scattering. UrQMD (ultra-relativistic quantum molecular dynamical model) [13] is a transport model based on the same principles as RQMD, but it incorporates vastly extended collision terms with full baryon-antibaryon symmetry, 55 baryon and 32 meson species. Isospin is explicitly treated for all hadrons. The three models have different physical mechanisms and will be helpful for us to understand the correlation patterns from different physical mechanisms.

### 2.2 Centrality dependence

Figure 1 shows the centrality dependence of rapidity correlation patterns for Au+Au collisions at $\sqrt{s_{\rm NN}}$=200 GeV. Due to the existing data samples, rapidity is used for AMPT and RQMD, pseudorapidity is used for UrQMD. We choose all charged particles in the (pseudo)rapidity range [−3, +3]. The (pseudo)rapidity range is divided equally into 30 bins.

In the upper panels of Fig. 1, the results of AMPT with string melting are shown. It is observed that the correlation strength decreases as the Au+Au collisions become more and more central, and correlation patterns become less dependent on the positions of the bins. These correlation patterns are consistent with those generated by AMPT with string melting at the same collision energy $\sqrt{s_{\rm NN}}$=200 GeV in Ref. [8], which are the expected correlation patterns if QGP is formed, as argued there. However, in the middle panels and lower panels of Fig. 1, the RQMD and UrQMD results are in exactly the same trend as those observed in AMPT with string melting, i.e. the correlation patterns become smaller and flatter in central collisions. As we introduced above, RQMD and UrQMD are hadron based transport models, where parton interaction is absent. So, little position dependence of correlation patterns does not require parton interaction, or the formation of QGP, in contrast to the conclusions from the models with QGP [8, 10] and data [4].

The behaviors of SRC are reflected in the neighboring bin correlation patterns, shown in the first column of Fig. 1. It is observed that SRC is the strongest in the central rapidity region ($y$=0), and drops slowly from the central to edge rapidity. SRC also drops

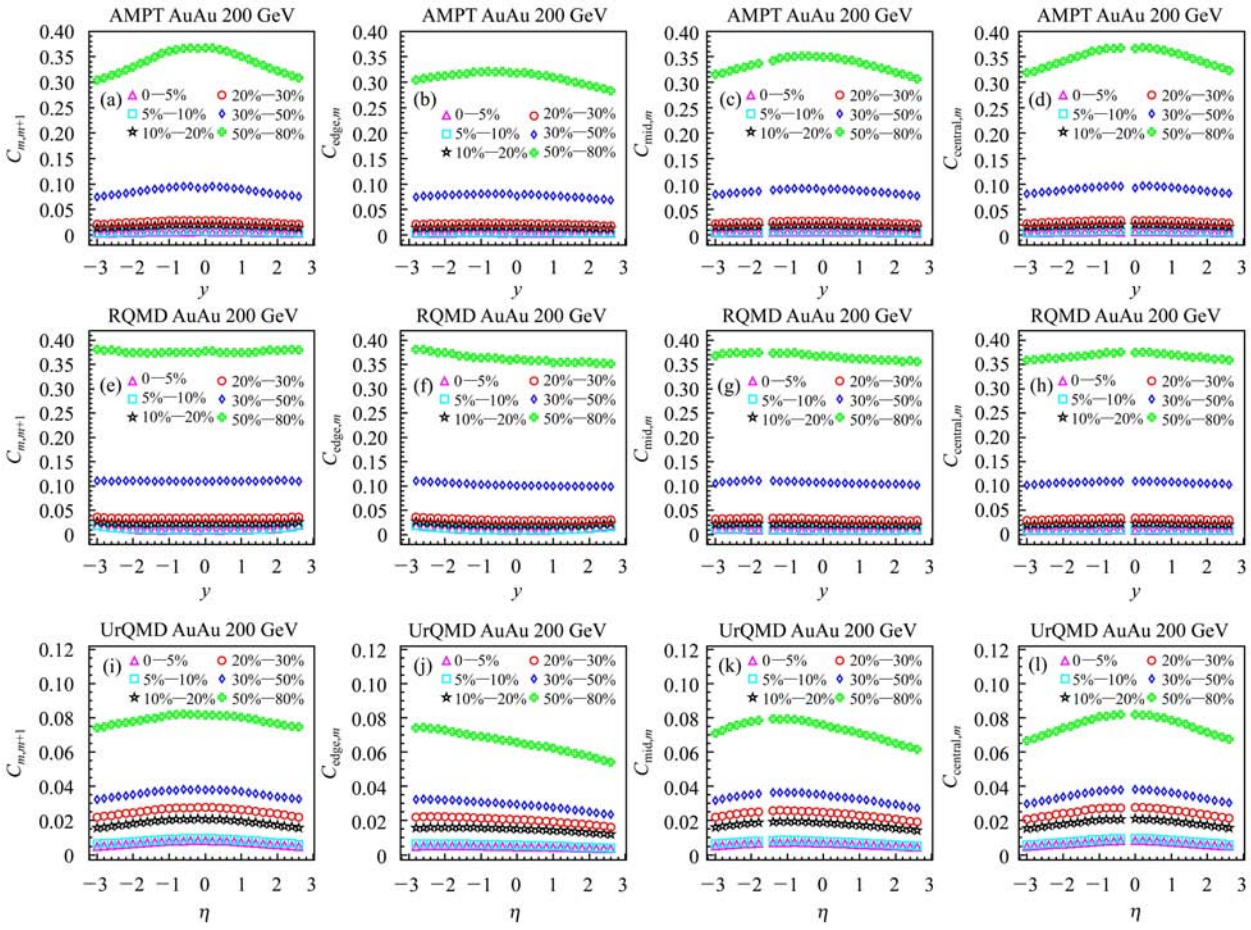


Fig. 1. (Color online) The neighboring bin and the fixed-to-arbitrary bin (pseudo) rapidity correlation patterns for Au+Au collisions at $\sqrt{s_{\mathrm{NN}}}$=200 GeV in several centralities. The upper panels are correlation patterns from AMPT with string melting, the middle panels are from RQMD and the lower panels are from UrQMD for comparison. Centrality is selected by the impact parameter.

from peripheral to central collisions and falls to a minimum in most central events.

In the other three columns of Fig. 1, the fixed-to-arbitrary bin correlation patterns are shown, with a fixed bin in the edge rapidity, mid rapidity and central rapidity. For example, if the rapidity range $[-3, +3]$ is divided equally into 30 bins, the fixed bins in $C_{\mathrm{edge},m}$, $C_{\mathrm{mid},m}$, $C_{\mathrm{central},m}$ are bins 1, 8, 15, corresponding to $y=-2.9$, $y=-1.5$, $y=-0.1$, respectively. We observe that the correlation patterns change with both correlation length and bin position. As the collisions become more and more central, the correlation patterns become more and more flat, and the correlation range is extended further and further, i.e. long range rapidity correlation appears in the central collisions. As discussed in Section 1, the dual parton model and the color glass condensate [4] argued that long range rapidity correlation is caused by the interactions at parton level. Our results from RQMD and UrQMD again reproduce the LRC. So the interaction at parton level is not the unique source of long range correlation; the rescattering and transportation at hadron level can lead to the long range rapidity correlation as well.

On the other hand, the centrality dependence of rapidity correlation patterns

$$C_{m_1,m_2}=\frac{\langle n_{m_1}n_{m_2}\rangle-\langle n_{m_1}\rangle\langle n_{m_2}\rangle}{\langle n_{m_1}\rangle\langle n_{m_2}\rangle}$$

from the models show opposite trend to forward-backward multiplicity correlations

$$b=\frac{\langle N_{\mathrm{f}}N_{\mathrm{b}}\rangle-\langle N_{\mathrm{f}}\rangle\langle N_{\mathrm{b}}\rangle}{\langle N_{\mathrm{f}}^2\rangle-\langle N_{\mathrm{f}}\rangle^2}$$

from experiment [4]. Experimental results show that the more central the collision, the stronger the correlation, while the results from AMPT, RQMD and UrQMD demonstrate that the more central the collision, the smaller the correlation. It is difficult to understand the reason at first glance. In fact, the correlation strength from two measures cannot compare because they are normalized differently, i.e. the first is normalized by the average while the latter is

normalized by dispersion. The average of multiplicity grows quickly from peripheral to central while the numerator may vary slowly, which leads to the decrease in correlation observable from peripheral to central.

## 3 Energy dependence of rapidity correlation patterns

We choose all charged particles for Au+Au collisions. The rapidity ranges used are listed in Table 1. Then the rapidity range is divided equally into several bins.

Table 1. Beam rapidity and the rapidity range used in this analysis.

| colliding energy/GeV | beam rapidity | rapidity range |
|---|---|---|
| 200 | 5.297 | (−3, 3) |
| 62.4 (60) | 4.134 (4.084) | (−3, 3) |
| 7.7 | 2.024 | (−1.8, 1.8) |

The results are shown in Fig. 2. The behaviors of SRC are reflected in the neighboring bin correlation patterns, shown in the first column in Fig. 2. In AMPT, at high energy, SRC is the strongest in the central rapidity region ($y$=0) and drops from the central to edge rapidity, i.e. SRC strongly depends on the bin positions. As the energy decreases, the magnitude of SRC also drops. When arriving at 7.7 GeV, a nearly flat correlation structure is presented, which means that SRC becomes not dependent on the bin positions. In RQMD it is quite different. SRC shows a flat structure at high energy, having no dependence on the positions of the bins, and changes to a narrow distribution at low energy, becoming obviously dependent on the positions of the bins.

In the other three columns of Fig. 2, the fixed-to-arbitrary bin correlation patterns are shown, with the fixed bin in the edge, mid and central rapidity. The correlation structures also show collision energy dependence and are still sensitive to models. It is interesting to see that the correlation patterns in RQMD at low collision energies are similar to those in AMPT at high collision energies, i.e. a convex curve shows strong position dependence. In contrast, the correlation patterns in RQMD at high collision energies and those in AMPT at low collision energies both show flat structures and have no position dependence.

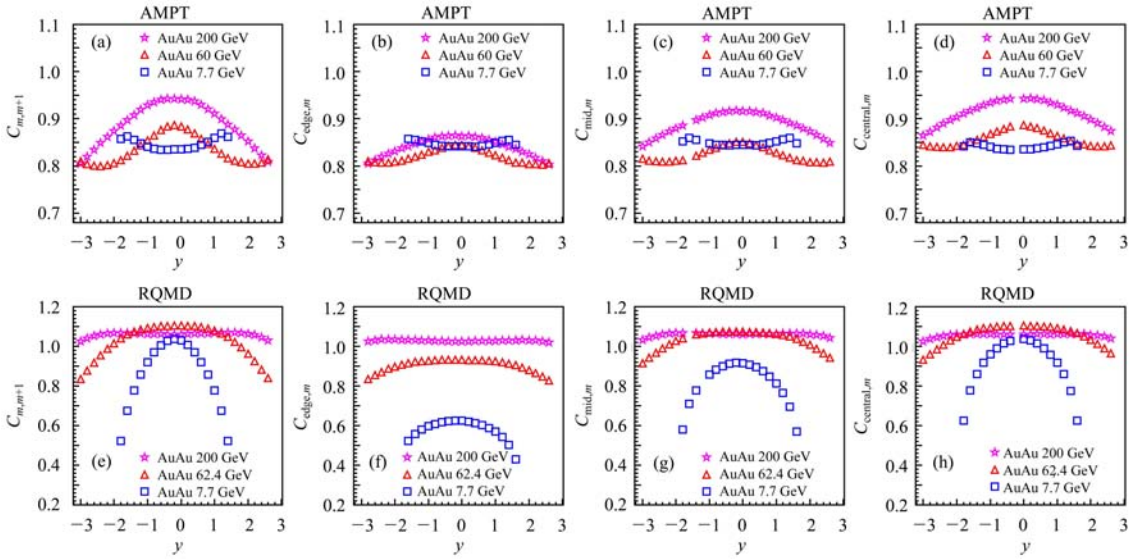


Fig. 2. (Color online)The neighboring bin and the fixed-to-arbitrary bin rapidity correlation patterns for minibias Au+Au collisions at several energies. The upper panels are correlation patterns from AMPT; the lower panels are from RQMD for comparison.

In order to clearly show how the correlation strength changes with the correlation length, we plot the variation in $C_{\mathrm{central},m}$ with $\Delta y$ in Fig. 3. $C_{\mathrm{central},m}$ presents the correlation of the central rapidity-bin ($y$=0) to another rapidity-bin, $\Delta y$ denotes the correlation length. This time we see clearly that $C_{\mathrm{central},m}$ shows dependence on correlation length in AMPT at high energy $\sqrt{s_{\mathrm{NN}}}$=200 GeV, i.e. the value of $C_{\mathrm{central},m}$ decreases with $\Delta y$. As the energy decreases, the correlation strength also drops. At energy $\sqrt{s_{\mathrm{NN}}}$=7.7 GeV, the correlation becomes flat. However, we cannot make some statements about the correlation length even though it exhibits a flat structure and may have a further correlation range since the rapidity range at low energy is cut.

In RQMD, from 200 GeV to 7.7 GeV, the cor-

relation patterns become more and more narrow in rapidity phase space and the correlation range gradually diminishes. Long range correlation presents itself at high energy and disappears at low energy. The origin of LRC in RQMD at high energy is still unknown. Anyhow, it is not parton interaction.

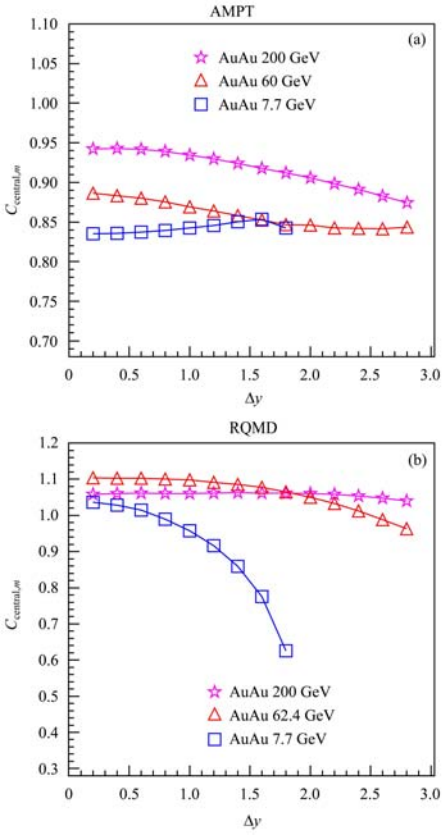


Fig. 3. The variation in $C_{\mathrm{central},m}$ with $\Delta y$ for Au+Au by AMPT and RQMD.

For the strength of correlation, in Fig. 3, AMPT exhibits larger SRC (see the value near $\Delta y \approx 0$) at high energy than low energies, while in RQMD a nearly constant value of SRC is shown at all energies.

## 4 Summary

We study the centrality and energy dependence of rapidity correlation patterns in Au+Au collisions by using AMPT with string melting, RQMD and UrQMD models. The centrality dependences of rapidity correlation patterns in UrQMD and RQMD are similar to those in AMPT with string melting, i.e. in most central collisions the correlation structure is flatter and the correlation range is larger, which indicates a long range rapidity correlation. This shows that the interaction at the parton level is not the only source of long range rapidity correlations.

The behaviors of the energy dependence of rapidity correlation patterns are quite different in AMPT with string melting and RQMD. The correlation patterns in RQMD at low collision energies and those in AMPT at high collision energies have similar structures, i.e. a convex curve, while the correlation patterns in RQMD at high collision energies and those in AMPT at low collision energies show flat structures and have no position dependence. The narrowing of correlation patterns in RQMD at low collision energies shows that SRC is dominant, while in RQMD at high collision energy the long range correlation shows up. This implies that long range rapidity correlations may come from some trivial effects, rather than the parton interactions.

We also discuss the difference between $C_{m_1,m_2}$ and $b$. $C_{m_1,m_2}$ measuring the correlation between two arbitrary bins in the phase space while $b$ focuses on two symmetric bins with respect to $y = 0$. Although they have the same measure at the numerator, the denominators are quite different, which leads to the different energy and centrality dependence.

*We express our gratitude to Wang Mei-Juan and Wu Ke-Jun for helpful discussions, and Zhou You and Li Na for sharing the data sample.*

## References

1 Hanbury Brown R, Twiss R Q. Nature (London), 1956, **178**: 1046; Shuryak E. Phys. Lett. B, 1973, **44**: 387; Sov. J. Nucl. Phys., 1974, **18**: 667
2 Paladin G, Vulpiani A. Phys. Rep., 1987, **156**: 147; Bialas A, Peschanski R. Nucl. Phys. B, 1988, **308**: 857
3 Seibert D. Phys. Rev. D, 1990, **41**: 3381; Bass S A, Danielewicz P, Pratt S. Phys. Rev. Lett., 2000, **85**: 2689
4 Abelev B I et al. (STAR collaboration). Phys. Rev. Lett., 2009, **103**: 172301; Srivastava B K (STAR collaboration). Int. J. Mod. Phys. E, 2007, **16**(10): 3371
5 Bozek P, Ploszajczak M, Botet R. Phys. Rep., 1995, **252**: 101
6 WU Yuan-Fang, LIU Lian-Shou, WANG Ying-Dan, BAI Yu-Ting, LIAO Hong-Bo. Phys. Rev. E, 2005, **71**: 017103
7 WANG Mei-Juan, WU Yuan-Fang. HEP&NP, 2006, **30**(7): 652 (in Chinese)
8 WANG Mei-Juan, WU Yuan-Fang. Int. J. Mod. Phys. E, 2007, **16**(10): 3379
9 Adams J et al. (STAR collaboration). Phys. Rev. C, 2006, **73**: 064907; 2007, **75**: 034901
10 YAN Yu-Liang et al. arXiv:1001.1595v1[nucl-th]
11 LIN Zi-Wei, KO Che-Ming, LI Bao-An, ZHANG Bin, Pal Subrata. Phys. Rev. C, 2005, **72**: 064901
12 Sorge H. Phys. Rev. C, 1995, **52**: 3291
13 Bass S A et al. arXiv:nucl-th/9803035v2